Springer

Journal of
Mechanical
Science and
Technology

Journal of Mechanical Science and Technology 23 (2009) 3292~3301

www.springerlink.com/content/1738-494x
DOI 10.1007/s12206-009-0807-4

Rolling element bearing fault detection using an improved combination of Hilbert and Wavelet transforms

Dong Wang, Qiang Miao*, Xianfeng Fan and Hong-Zhong Huang

School of Mechanical, Electronic, and Industrial Engineering, University of Electronic Science and Technology of China Chengdu, Sichuan, China, 610054

(Manuscript Received March 11, 2009; Revised July 28, 2009; Accepted August 6, 2009)

Abstract

As a kind of complicated mechanical component, rolling element bearing plays a significant role in rotating machines, and bearing fault detection benefits decision-making of maintenance and avoids undesired downtime cost. However, extraction of fault signatures from a collected signal in a practical working environment is always a great challenge. This paper proposes an improved combination of the Hilbert and wavelet transforms to identify early bearing fault signatures. Real rail vehicle bearing and motor bearing data were used to validate the proposed method. A traditional combination of Hilbert and wavelet transforms was employed for comparison purpose. An indicator to evaluate fault detection capability of methods was developed in this research. Analysis results showed that the extraction capability of bearing fault signatures is greatly enhanced by the proposed method.

Keywords: Rolling element bearings; Hilbert transform; Wavelet transform; Fault detection; Fault detection capability evaluation

1. Introduction

Rolling element bearings are widely used in many industrial fields to provide support of shafts. The health condition of bearings affects the desired output of machines. However, bearings are prone to failure due to many factors such as incorrect design or installation, corrosion, poor lubrication and plastic deformation [1]. As a result, bearings frequently have local defects including cracks, pits and spalls on the surfaces of raceways, cage, and rollers. Serious bearing fault may cause unplanned breakdown and accidents, and destroy the decision-making plan of maintenance as well. Therefore, fault detection and diagnosis of bearings in rotating machines is significant. However, it is a great challenge to extract early bearing fault signatures from collected signals because (a) components such as inner races, outer races, rollers, and cages in a rolling element bearing result in the complication of bearing vibration signals, and (b) the collected signal is always polluted by background noise and mixed with vibration signals of shafts, gears, and other mechanical components.

If a failure occurs on a working surface of bearing elements, impact will be generated when a mating element encounters the failure one. Sharp transient response accompanied by damped oscillation should occur in measured vibration signals. The information of bearing condition is expected to be extracted from this transient behavior in vibration signals. In addition, the observed signal may present a modulation phenomenon caused by the resonance vibration stimulated by a bearing failure and bursts of exponentially decaying vibration. Bearing fault features may be extracted from a spectrum analysis of the signal envelope (i.e., the spectrum of the bursts of exponentially decaying vibration). However, direct spectrum analysis of the envelope of a raw signal may not always be

† This paper was recommended for publication in revised form by Associate Editor Hong Hee Yoo

*Corresponding author. Tel.: +86 28 6183 1669, Fax.: +86 28 6183 0229
E-mail address: mqiang@uestc.edu.cn

effective because of the complexity of the collected signal. Therefore, researches have been conducted to focus on the envelope analysis from the signal located in certain specific frequency bandwidth. Jiménez et al. [2] used Hilbert and Wavelet transforms to make the fault diagnosis easier.

Wavelet analysis is able to decompose a signal into different scales corresponding to different frequency bandwidth [3] and has been used to extract machine fault signatures. Miao et al. [4] evaluated machine health condition based on wavelet transform and extracted a quantitative description of whole life rotating machinery. Sun and Tang [5] employed continuous wavelet transform (CWT) to detect abrupt changes in bearing vibration signals. Unfortunately, many samples are needed to obtain enough bearing signatures because the frequency ranges of the bearing vibration signals are usually wide, which requires a high sampling frequency according to the Shannon sampling theorem [6-7]. In addition, enough CWT scales should be adopted to catch the desired frequency resolution. Therefore, CWT may be time consuming to analyze bearing vibration signal. Discrete wavelet transform (DWT) comes from the discretization of CWT scales. Mori et al. [8] analyzed the approximation and detail coefficients of the DWT for bearing fault detection. Prabhakar et al. [9] also employed DWT to detect single and multiple faults in ball bearings. Therefore, wavelet analysis may have the potential to further extract signatures from the a signal located in specific frequency bands with the help of Hilbert spectrum analysis. Tse et al. [10] proposed a method of wavelet analysis and FFT with envelope detection to extract bearing faults. Jiménez et al. [2] used Hilbert and wavelet transforms to detect faults in induction motors. Fan and Zuo [11] proposed a method based on Hilbert and wavelet packet transforms to detect gear faults. However, the accessible literatures on bearing fault detection using Hilbert and wavelet transforms are very limited. Additionally, some potential advantages of Hilbert transform for fault detection have not been fully developed and employed yet.

With the motivation to improve the capability of bearing fault detection, a signal analysis method based on Hilbert and wavelet transforms is proposed in this study, which applies the Hilbert transform twice. The rest of this paper is organized as follows. In section 2, both Hilbert and wavelet transforms are briefly introduced. A potential benefit of Hilbert transform is discussed. An improved method for bearing fault detection is proposed in Section 3. In Section 4, the real vibration data of both rail vehicle bearing and motor bearing are used to evaluate the proposed method. An indicator to evaluate the fault detection capability of these methods is proposed as well. A comparison study is conducted to demonstrate the advantages of the proposed method. Finally, conclusions and discussion are given.

2. Brief review of Hilbert and wavelet transforms

2.1 Hilbert transform

Assume a piece of signal $x(t)$ and its Hilbert transform $H[x(t)]$ which is defined as [12-13]:

$$H[x(t)] = \frac{1}{\pi}\int_{-\infty}^{+\infty}\frac{x(\tau)}{t-\tau}d\tau \tag{1}$$

where t and τ are time and translation parameters, respectively. It is well known that the Hilbert transform is a time-domain convolution that maps one real-valued time-history into another and it is also a frequency-independent 90° phase shifter. So, it does not influence the non-stationary characteristics of modulating signals. In actual application, modulation is usually caused by machine faults. Hence, in order to find fault related signatures, demodulation has to be done. Fortunately, this requirement may be completed by construction of analytic signal, which is given by

$$B(t) = x(t) + iH[x(t)] = b(t)e^{\phi(t)} \tag{2}$$

where $b(t) = \sqrt{x^2(t) + H^2[x(t)]}$, $\phi(t) = \arctan\dfrac{H[x(t)]}{x(t)}$, and $i = \sqrt{-1}$. $b(t)$ is the envelope of $B(t)$.

The Fourier transform of signal $B(t)$ is notified by $\hat{B}(i\omega)$ and its properties are provided as [14]:

$$\hat{B}(i\omega) = \begin{cases} 2\hat{x}(i\omega) & 0 \le \omega \\ 0 & \omega < 0 \end{cases} \tag{3}$$

where ω denotes the angular frequency of $\hat{B}(i\omega)$ and $\hat{x}(i\omega)$ is Fourier transform of $x(t)$.

On one hand, the Hilbert transform can demodulate modulated signals and extract modulating signals. On the other hand, we observe in our research that the

spectrum analysis of an envelope signal obtained from an analytic signal is able to enhance the amplitude of an original signal by Eq. (3), which may be useful to increase the amplitude of bearing fault signatures for visual inspection. To explore the potential of the Hilbert transform in bearing fault detection, a simulated signal is analyzed, which is given as follows:

$$x(t)=\sum_{k=0}^{4}20\sin(350\cdot(t-0.201k)\cdot e^{-60(t-0.201k)} +rand(t)\quad t=[0,1] \tag{4}$$

where k is an integer, and $rand(t)$ denotes a normally distributed white noise. $20\sin(350\cdot(t-0.201k)\cdot e^{-60(t-0.201k)}$ is used to simulate the impulse signal. The time interval between every two adjacent impulses is 0.201 second which corresponds to a characteristic frequency of 1/0.201=4.975 Hz.

The impulse signal, noise, and their mixture are plotted in Figs. 1(a)-(c), respectively. We then analyze the mixed signal in Fig. 1(c) using two methods: (1) perform the spectrum analysis of the envelope obtained by Hilbert transform once, and (2) perform the spectrum analysis of the envelope obtained by Hilbert transform twice. The analysis results obtained by both of the above methods are shown in Fig. 2. Though the amplitudes of the Hilbert transform twice are not exactly the double of those of single Hilbert transform, it is able to find that the amplitude of the result using Hilbert transform twice is obviously higher than that of the result obtained by Hilbert transform once at the characteristic frequency 4.975 Hz and its harmonics. This demonstrates that the implementation of the Hilbert transform twice can enhance the amplitudes located at the characteristic frequency and its harmonics. We also notice that the changes of other frequency components are too weak to be ignored. This priority may have great potential to extract bearing fault signatures.

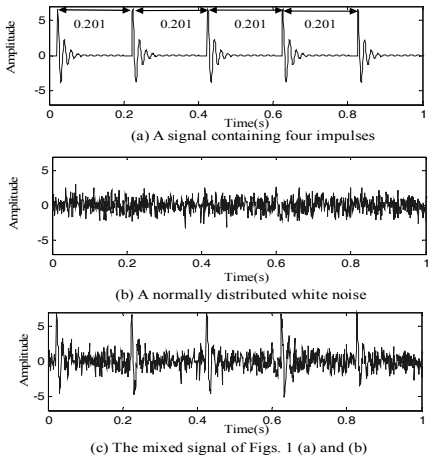

Fig. 1. The simulated signals.

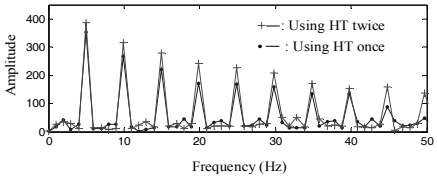

Fig. 2. The spectrum analysis of the envelopes obtained by Hilbert transform once and twice, respectively.

2.2 Wavelet transform

Continuous wavelet transform of a finite-energy signal can be defined as the integral of a signal $x(t)$ multiplied by scaled and shifted versions of a basic wavelet function $\psi(t)$ [3], as:

$$W(a,b)=\int_R x(t)\frac{1}{\sqrt{a}}\psi^*(\frac{t-b}{a})dt \quad a\in R^+, b\in R \tag{5}$$

where R^+ and R are the positive real number and real number, respectively. a and b are the scaling parameter and the translation parameter, respectively. $*$ means the conjugate operation. The Fourier transform of $\psi(t)$ satisfies the following admissibility criteria [3]:

$$C_\psi=\int_R d\omega|\hat{\psi}(\omega)|^2|\omega|^{-1}<\infty \tag{6}$$

where $\hat{\psi}(\omega)$ denotes the Fourier transform of $\psi(t)$.

According to Eq. (5), we know that $W(a,b)$ is defined on an a-b plane, where a and b are used to adjust the frequency and time location of wavelet $\psi(t)$ by:

$$\psi_{(a,b)}(t)=\frac{1}{\sqrt{a}}\psi(\frac{t-b}{a}) \quad a\in R^+, b\in R \tag{7}$$

Here, $\sqrt{a}$ is used for energy preservation. A small parameter a corresponds to high-frequency components. Parameter b represents the location of wavelet function in time domain. According to Eq.

(5), wavelet coefficient $W(a,b)$ is able to measure the similarity between signal $x(t)$ and wavelet $\psi(t)$ at different frequencies determined by scale parameter a and different time locations determined by parameter b.

Discrete wavelet transform is derived from CWT, where scales and positions are commonly chosen based on a power of 2, i.e., dyadic scale and positions [15], through

$$a = 2^j, b = k2^j, \qquad j,k = \{0,\pm1,\pm2,...\}. \tag{8}$$

The discrete wavelet function and the scaling function are defined as:

$$\psi_{j,k}(t) = 2^{-j/2}\psi(2^{-j}t - k) \tag{9}$$

$$\phi_{j,k}(t) = 2^{j/2}\phi(2^{-j}t - k) \tag{10}$$

DWT can be implemented by filter operation. The filters used in DWT contain a high-pass filter (wavelet filter) and a low-pass filter (scaling filter) that are constructed, respectively.

$$g(n) = \frac{1}{\sqrt{2}}\langle\psi(t),\psi(2t-n)\rangle = (-1)^n h(1-n) \tag{11}$$

$$h(n) = \frac{1}{\sqrt{2}}\langle\phi(t),\phi(2t-n)\rangle \tag{12}$$

A fast wavelet transform proposed by Mallat [15] is able to perform two opposite operations: decomposition and reconstruction. In decomposition, a discrete signal is convolved with a low pass filter and a high pass filter, respectively. Letting $x(t) = A_0(t)$, the decomposition process can be repeated as follows

$$A_{j-1}(t) = A_j(t) + D_j(t), \tag{13}$$

where $A_j(t)$ and $D_j(t)$ are called approximation and detail at the Jth decomposition level, respectively. In reconstruction, a pair of low-pass and high-pass reconstruction filters are convolved with $A(t)$ and $D(t)$, respectively.

The wavelet tree of wavelet decomposition at level 4 is shown in Fig. 3. $A_j(t)$ includes $N/2^j$ coefficients, where N is the length of signal $x(t)$. The information obtained by DWT on each scale corresponds to a frequency bandwidth $F_s/2^{j+1}$, where F_s is a sampling rate. The original signal can then be reconstructed by the sum of $A_j(t)$ and $D_j(t)$ by Eq. (13). It is also easy to obtain a reconstructed signal in a desired frequency bandwidth by setting wavelet transform coefficients beyond the desired frequency bandwidth to zero.

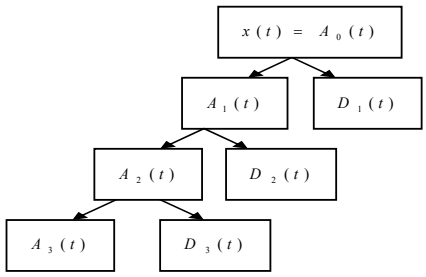

Fig. 3. An example of a four-level wavelet decomposition tree.

3. The proposed method for bearing fault signature extraction

For a collected signal $y(t)$, a pre-process is necessary to relieve the influence of random variables before the proposed method. This process can be implemented as

$$x(t) = \frac{y(t) - \bar{y}}{\sigma} \tag{14}$$

where $x(t)$ is the pre-processed signal, $\bar{y}$ is the mean value of $y(t)$, and σ denotes the standard deviation of $y(t)$.

In bearing fault detection, the amplitude of the envelope spectrum of a normal bearing is distributed randomly and evenly over the entire frequency domain. On the other hand, for a faulty bearing, the amplitudes of a characteristic frequency and its harmonics become dominant over other frequency components [16]. The modulated signal can be demodulated by using Eq. (2), and thus the fault related signatures can be exhibited. To better explore fault-related information, DWT can be used to divide finer frequency ranges. The flow chart of the proposed method in this paper is shown in Fig. 4, which includes following steps:

Step 1. Load an original signal $y(t)$ and preprocess it to obtain $x(t)$ by Eq. (14). Perform Hilbert transform to obtain the analytic signal of $x(t)$, and extract the envelope signal.

Step 2. Decompose the envelope obtained in step 1 using DWT.

Step 3. Because the resonant vibration existing in a high frequency bandwidth may be stimulated by a bearing fault, the detail signals are chosen to extract fault characteristics. Reconstruct detail signals $D_j(t)$ based on the wavelet coefficients obtained in Step 2.
Step 4. Perform Hilbert transform of all reconstructed signals in high frequency bandwidth to obtain the analytic signals located in different high frequency bandwidth.
Step 5. Perform spectrum analysis of envelope $b_{2\_j}(t)$ corresponding to $D_j(t)$.
Step 6. Select the optimal envelope spectrum from those obtained in Step 5.
Step 7. Identify bearing characteristic frequency and its harmonics.

There are many wavelets available, and Morlet wavelet [17-18] and Daubechies wavelet were commonly used when performing wavelet transform. For instance, the research of Prabhakar [9] and Fan and Zuo [11] showed the feasibility of Daubechies wavelets. Prabhakar et al. employed DWT to find ball bearing race faults at the fourth level. Fan and Zuo used the combination of Hilbert transform and wavelet packet to diagnose gearbox faults at the fourth decomposition level. For the same reason, Daubechies wavelet is utilized to analyze vibration signals and decomposition level is established at four.

Similar to the idea of Fan et al. [16], an improved envelope spectrum amplitude index is proposed to select the optimal envelope spectrum of all $Z_j(t)$, $j=1,2,\cdots,J$, in step 6.

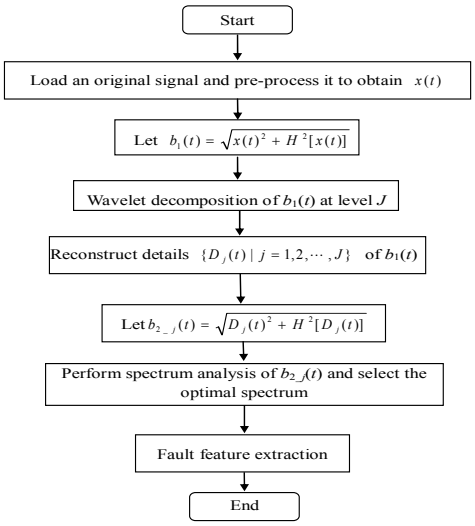

Fig. 4. The flow chart of the proposed method.

First, to reduce the undesirable end effects of a signal envelope, a new envelope signal is obtained:

$$E_j(t)=\left|Z_j(t)\right|-\frac{\sum\left|Z_j(t)\right|}{N} \tag{15}$$

where N presents the length of $Z_j(t)$.
Secondly, a spectrum analysis of $E_j(t)$ is performed by:

$$ES_j(f)=\left|\int_{-\infty}^{+\infty}E_j(t)e^{-2ift\pi}dt\right| \tag{16}$$

In Eq. (16), $ES_j(f)$ denotes the absolute value of the Fourier transform amplitude of the new envelope obtained by Eq. (15). The characteristic frequency and its harmonics become dominant in the frequency domain when bearing faults occur. Comparison with normal bearing shows that the total summation of the envelope spectrum increases dramatically for a faulty bearing. Therefore, for each $ES_j(f)$, it is feasible to use both $\max\{ES_j(kf^*)\mid k=1,2,\cdots,5\}$ and $\sum_{f=f^*,2f^*,\cdots,5f^*}ES_j(f)$ to express an obvious fault characteristic frequency in the frequency domain and total contribution caused by fault characteristic frequency and its harmonics, respectively. Usually, integer k is suggested from 1 to 5. f^* represents the fault characteristic frequency. k means the harmonic order of f^*. This provides an optional way to select optimal Z_j, which contains the most valuable information explained above. Hence, the envelope spectrum amplitude index is defined by:

$$\begin{aligned}ESI_j&=\log_{10}\{\max\{ES_j(kf^*)\mid k=1,2,\cdots,5\}\\&\times\sum_{f=f^*,2f^*,\cdots,5f^*,}ES_j(f)\}\quad j=1,2,\cdots,J\end{aligned} \tag{17}$$

In typical application, rolling elements in a bearing may slide and the machine speed may have some fluctuation. Thus, f^* may not exactly match the calculated value based on the size and parameters of bearings. Therefore, we focus on both $f^*\pm 2$ Hz and $k\times(f^*\pm 2)$ in this study and the logarithm format is used in Eq. (17). Therefore, the largest ESI_j can be used to select the optimal envelope spectrum of Z_j for fault signature extraction.

Then, the optimal envelope spectrum $ES(f)$ of $Z_j(t)$ by Eq. (17) is obtained. It can also be found

that the amplitudes at the bearing fault characteristic frequency and its harmonics should be enhanced compared with those obtained by the traditional combination methods of Hilbert and wavelet transforms, in which Hilbert transform was used only once.

To evaluate the capability of the proposed method, an indicator is proposed in this paper. The construction of the proposed indicator is as follows:

(1) Obtain the mean value of the summation of envelope spectrum:

$$\overline{E} = \frac{1}{M}\sum_{f=0}^{M-1} ES(f) \tag{18}$$

where M represents the length of the envelope spectrum, and $ES(f)$ denotes the envelope spectrum obtained by the proposed method or traditional combination of Hilbert and wavelet transforms.

(2) Choose the biggest amplitudes located at the fault characteristic frequency such as $f^* \pm 2$ Hz and its harmonics $k \times (f^* \pm 2)$. The biggest amplitude is denoted by $A_{k \times f^*}$.

(3) The proposed indicator is defined by:

$$Ind(k) = \frac{A_{k \times f^*}}{\overline{E}} \tag{19}$$

4. Case studies

4.1 The rail vehicle bearing fault detection

In the first experiment, a set of real bearing data was obtained through rail vehicle bearings running on a test rig. The sampling frequency was 32768 Hz. The length of each data set was 32768 points. Table 1 shows specifications of bearings. The rotating speed of the bearing shaft was $f_{rr} = 9.5$ Hz. The characteristic frequencies of bearing faults are calculated by using the equations in [19] and are shown in Table 2. The parameters have the same meaning as those in Table 1.

The raw signals collected from a normal bearing, a bearing with a serious inner race fault, and a bearing with an early outer race fault, are shown in Figs. 5(a)-(c) respectively. As we explained previously, Daubechies-9 wavelet was selected in this research for signal analysis and synthesis. The decomposition level is fixed as four.

Table 1. Rail vehicle bearing specifications.

Number of rollers	23
Contact angle β (deg)	9
Pitch diameter D (mm)	203
Mean roller diameter d (mm)	21.4

Table 2. The characteristic frequencies of rail vehicle bearing faults.

Bearing components	Characteristic frequencies (Hz)
Bearing components	$f_{rC} = \frac{f_{rr}}{2}(1 - \frac{d}{D}\cos\beta) = 4.25$
Inner race frequency	$f_{rI} = \frac{nf_{rr}}{2}(1 + \frac{d}{D}\cos\beta) = 120.63$
Outer race frequency	$f_{rO} = \frac{nf_{rr}}{2}(1 - \frac{d}{D}\cos\beta) = 97.87$
Rolling spin frequency	$f_{rR} = \frac{Df_{rr}}{2d}[1 - (\frac{d}{D}\cos\beta)^2] = 44.57$

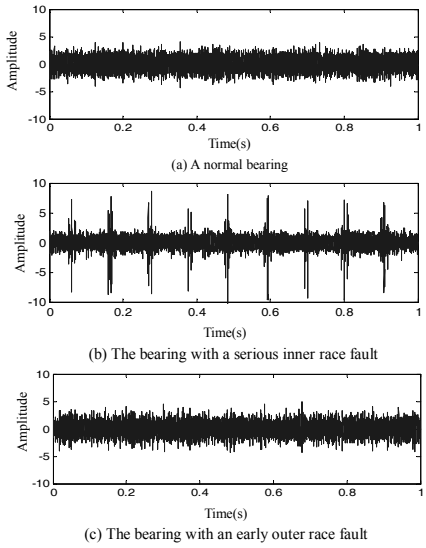

Fig. 5. The raw vibration signals of rail vehicle bearings.

When normal bearing data are analyzed firstly using the proposed method, the envelope spectra of $Z_1(t), Z_2(t), Z_3(t)$, and $Z_4(t)$, which correspond to $D_1(t), D_2(t), D_3(t)$, and $D_4(t)$, are plotted in Figs. 6(a)-(d), respectively. From the results obtained in Fig. 6, no fault characteristic frequency and its harmonics can be identified.

Then, the data of bearings with serious inner race fault are investigated; the envelope spectra of $Z_1(t)$, $Z_2(t)$, $Z_3(t)$ and $Z_4(t)$, which correspond to $D_1(t), D_2(t), D_3(t)$, and $D_4(t)$, obtained by the

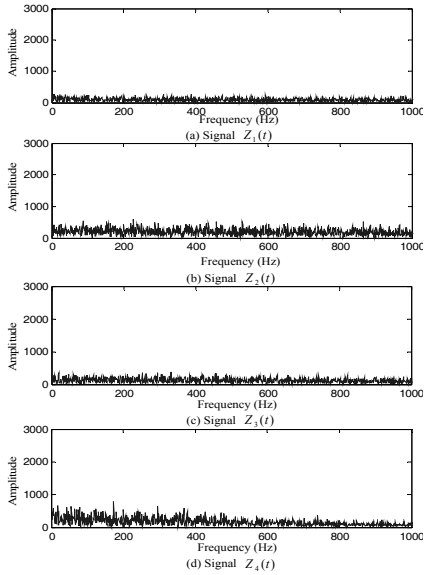

Fig. 6. The analysis results of the rail vehicle normal bearing obtained by the proposed method.

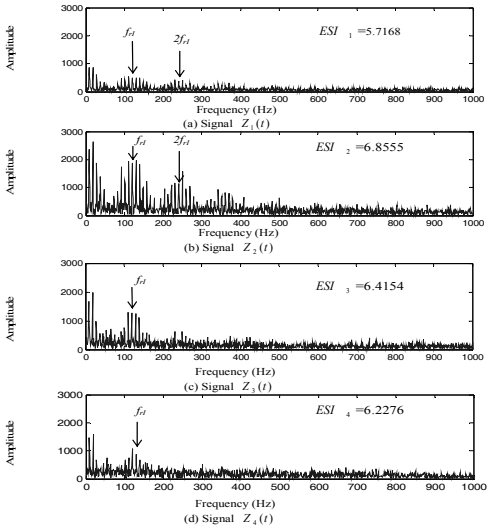

Fig. 7. The analysis results of the rail vehicle bearing with a serious inner race fault obtained by the proposed method.

proposed method are shown in Figs. 7(a)-(d), respectively. It is obvious that Fig. 7(b) contains the most fault-related signatures. The same results can be also gained through Eq. (17). After calculation, $ESI_2 = 6.8555$ is the largest value among all ESI_j.

The proposed method is extended to the data of bearings with an early outer race fault (Fig. 5(c)) at the fourth level with dB9. Fig. 8. shows the obtained results. $Z_1(t)$ with the biggest $ESI_1 = 6.5861$ is

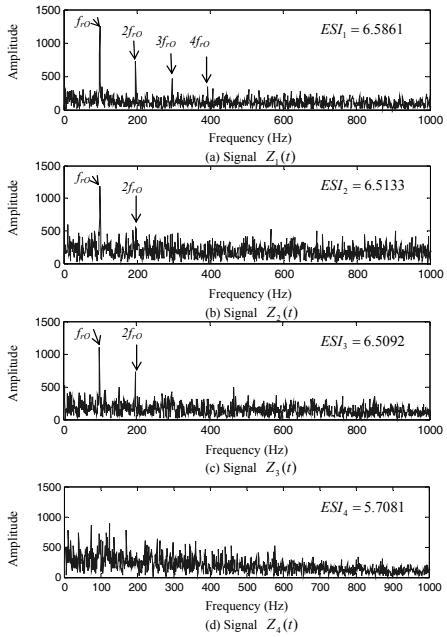

Fig. 8. The analysis results of rail bearing with an early outer race fault obtained by the proposed method.

selected to detect bearing fault signatures by using Eq. (17). Compared with Figs. 8(b)-(d), Fig. 8(a) shows the best performance in identification of characteristic frequencies, which proves that the proposed index is correct for choosing the most useful fault-related signatures.

For comparison, the traditional combination of Hilbert and Wavelet transforms (dB9 wavelet, DWT at the fourth level) is used in the study. Analysis results of bearings with outer race and inner race faults are shown in Fig. 9(a) and (b), respectively. In Fig. 9(a), fault characteristic frequency f_{rI} and its second harmonics are dominant in the frequency domain. Other harmonics are hardly visible. In Fig. 9(b), only the peaks at f_{ro} and $2f_{ro}$ are clear. It is hard to identify harmonics of f_{ro}. Therefore, the proposed method is better than the traditional method.

To further compare the effect of the two methods, a proposed indicator $Ind(k)$ is employed to quantitatively evaluate the capability of the fault diagnosis. Figs. 10 and 11 show the indicator for the bearing with a serious inner race fault and the indicator for the bearing with an early outer race fault, respectively. In Figs. 10 and 11, we can clearly find that the indicators obtained by the proposed method are larger than those obtained by the traditional method. This result shows

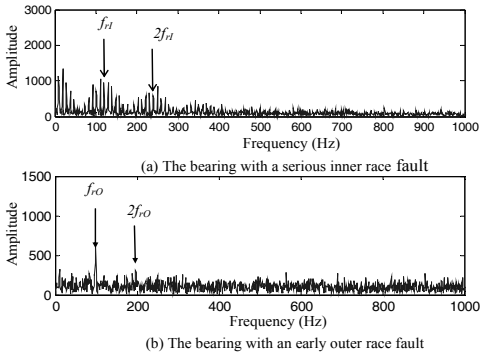

Fig. 9. The rail vehicle bearing analysis results obtained by the traditional combination of Hilbert and wavelet transforms (dB9wavelet, DWT at the fourth level).

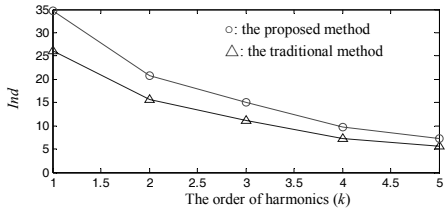

Fig. 10. The indicators for the rail vehicle bearing with a serious inner race fault.

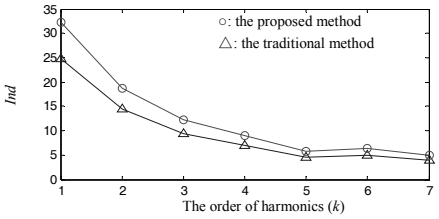

Fig. 11. The indicators for the rail bearing with an early outer race fault.

that the proposed method has better capability in bearing fault detection.

4.2 The motor bearing fault detection

To further verify the proposed method, the real motor bearing data picked up with a sampling frequency 12K Hz by an accelerometer placed at the 6 o'clock position at the drive end of the motor housing, is analyzed as well. Single point faults were introduced to normal bearings using electro-discharge machining with a fault diameter of 0.007 inches, and the fault depth was 0.0011 inches. The

Table 3. Motor bearing specifications (inches).

Inside Diameter	0.9843
Outside Diameter	2.0472
Thickness	0.5906
Ball Diameter	0.3126
Pitch Diameter	1.537

Table 4. The characteristic frequencies of motor bearing faults (Hz).

Inner race frequency	$f_{mI} = 5.4152 \times f_{mr}$ =160.02
Outer race frequency	$f_{mO} = 3.5848 \times f_{mr}$ =105.93
Cage frequency	$f_{mC} = 0.39828 \times f_{mr}$ =11.77
Rolling frequency	$f_{mR} = 4.7135 \times f_{mr}$ =139.28

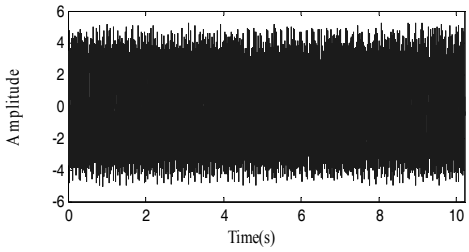

Fig. 12. The raw vibration signals of the motor bearing with an outer race fault.

specifications of bearings are shown in Table 3. The characteristic frequencies of the bearing are calculated in Table 4. The shaft speed of bearings is f_{mr} =29.55 Hz. The original vibration signal is shown in Fig. 12.

Wavelet analysis of the signal in Fig. 12 is performed using dB9 at the fourth level to obtain the detail signals D_1, D_2, D_3 , and D_4 . The envelope spectra of Z_1, Z_2, Z_3 , and Z_4 , which correspond to D_1, D_2, D_3 , and D_4 , are shown in Fig. 13. Z_1 with the biggest $ESI_1 = 8.3464$ will be selected.

The analysis results obtained by the traditional combination of Hilbert and Wavelet transforms (dB9 wavelet, DWT at the fourth level) are shown in Fig. 14 as well. In Fig. 14, we can extract the fault characteristic frequency at f_{mO} , and its harmonic also can be identified visually. To show the advantages of the proposed method in this paper, $Ind(k)$ is used in this section as well, shown in Fig. 15. We can clearly find the indicators using the proposed method are larger than those using the traditional method. This comparison indicates again that the proposed method can extract the fault signatures more effectively.

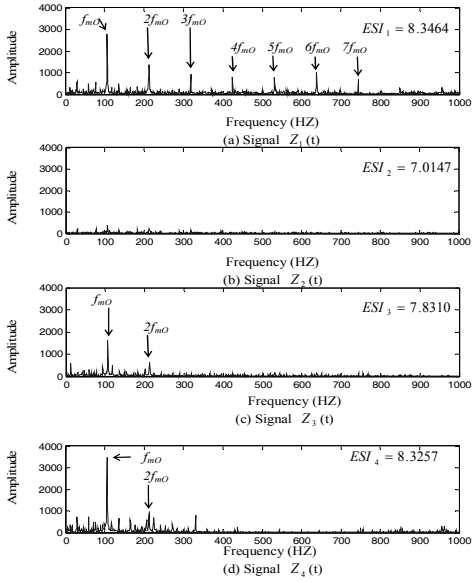

Fig. 13. The analysis results of the motor bearing with an outer race fault by the proposed method.

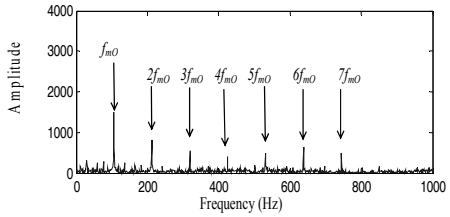

Fig. 14. The analysis results of motor bearing obtained by the traditional method.

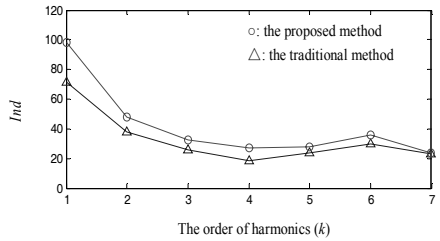

Fig. 15. The indicators for the motor bearing with an outer race fault.

5. Conclusion and future works

Even though the traditional combination of Hilbert and Wavelet transforms is able to detect bearing faults, it may exhibit poor performance in identification of fault-related signatures. To improve this method, a new combination of Hilbert transform and wavelet transform is proposed in this paper. In experimental study, both rail vehicle bearing and motor bearing data are employed to comprehensively validate the proposed method. Two indicators are proposed in this research. One is used to select the most useful detail signatures when DWT is performed. Another is used to evaluate the capability of the proposed method and the traditional method. The obtained results indicate that the proposed method has a better visual inspection than the traditional combination of Hilbert transform and wavelet transform. In other words, the proposed method improves the bearing fault detection capability to some extent and this benefit can help engineers identify bearing related fault signatures clearly. Finally, it should be pointed out that the proposed method focuses on the bearing fault detection with a fixed rotation speed at the fluctuation range of ±2 Hz. The fault detection of bearings working at greatly variable speed needs further research.

Acknowledgments

This research was partially supported by Specialized Research Fund for the Doctoral Program of Higher Education of China (Grant No. 20070614023), National Natural Science Foundation of China (Grant No. 50905028) and China Postdoctoral Science Foundation Funded Project (Grant No. 200801442). We are most grateful to Mr S. Chobsaard for providing the rail vehicle bearing data and Professor K. A. Loparo for his permission to use their bearing data in this research.

References

[1] V. Purushotham, S. Narayanan and S. A. N. Prasad, Multi-fault diagnosis of rolling bearing elements using wavelet analysis and hidden Markov model based fault recognition, *NDT&E Int.* 38 (8) (2005) 654-664.

[2] G. A. Jiménez, A. O. Muñoz and M. A. Duarte-Mermoud, Fault detection in induction motors using Hilbert and Wavelet transforms, *Electr. Eng.* 89 (3) (2007) 205-220.

[3] I. Daubechies, *Ten lectures on wavelets*, CBMS-NSF Series in Applied Mathematics (SIAM), Philadelphia, PA, (1992).

[4] Q. Miao, H. Z. Huang and X. F. Fan, Singularity detection in machinery health monitoring using Lipschitz exponent function, *J. Mech. Sci. Technol.* 21 (5) (2007) 737-744.

[5] Q. Sun and Y. Tang, Singularity analysis using continuous wavelet transform for bearing, *Mech.*

Syst. Signal Pr. 16 (6) (2002) 1025-1041.

[6] C. J. Li and J. Ma, Wavelet decomposition of vibrations for detection of bearing-localized defects, *NDT&E Int.* 30 (3) (1997) 143-149.

[7] P. D. McFadden and W. J. Wang, Analysis of gear vibration signatures by the weighted Wigner-Ville distribution, *Inter. Conference on Vibrations in Rotating Machinery*, Institution of Mechanical Engineers, Bath. (1992) 387-393.

[8] K. Mori, N. Kasashima, T. Yoshioka and Y. Ueno, Prediction of spalling on a ball bearing by applying the discrete wavelet transform to vibration signals, *Wear* 195 (1) (1996) 162-168.

[9] S. Prabhakar, A. R. Mohanty and A. S. Sekhar, Application of discrete wavelet transform for detection of ball bearing race faults, *Tribol. Int.* 35 (12) (2002) 793-800.

[10] P. W. Tse, Y. H. Peng and R. Yam, Wavelet analysis and envelope detection for rolling element bearing fault diagnosis-their effectiveness and flexibilities, *J. Vib. Acoust.* 123 (3) (2001) 303-310.

[11] X. F. Fan and M. J. Zuo, Gearbox fault detection using Hilbert and wavelet packet transform, *Mech. Syst. Signal Pr.* 20 (4) (2006) 966-982.

[12] A. Carcaterra and A. Sestieri, Complex envelope displacement analysis: a quasi-static approach to vibrations, *J. Sound Vib.* 201 (2) (1997) 205-233.

[13] G. Kerschen and A. F. Vakakis, Y. S. Lee, D. M. McFarland and L. A. Bergman, Toward a fundamental understanding of the Hilbert-Huang Transform in nonlinear structural dynamics, *J. Vib. Control* 14 (1-2) (2008) 77-105.

[14] H. Olkkonen, P. Pesola, J. Olkkonen and H. Zhou, Hilbert transform assisted complex wavelet transform for neuroelectric signal analysis, *J. Neurosci. Meth.* 151 (2) (2006) 106-113.

[15] S. Mallat, A theory for multiresolution signal decomposition: The wavelet representation, *IEEE T Pattern Anal.* 11 (7) (1989) 674-693.

[16] X. Fan, M. Liang, T. H. Yeap and B. Kind, A joint wavelet lifting and independent component analysis approach to fault detection of rolling element bearings, *Smart Mater. Struct.* 16 (5) (2007) 1973-1987.

[17] G.Y. Luo, D. Osypiw and M. Irle, On-line vibration analysis with fast continuous Wavelet algorithm for condition monitoring of bearing, *J. Vib. Control* 9 (8) (2003) 931-947.

[18] R. Bussow, An algorithm for the continuous Morlet wavelet transform, *Mech. Syst. Signal Pr.* 21 (8) (2007) 2970-2979.

[19] P. D. McFadden and J. D. Smith, Vibration monitoring of rolling element bearings by the high frequency resonance technique-a review, *Tribol. Int.* 17 (1) (1984) 3-10.

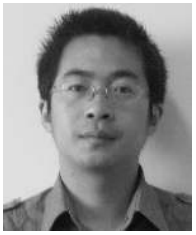

Dong Wang received his B.S. in Mechanical and Electronic Engineering from the University of Electronic Science and Technology of China. He currently is an M.S. candidate in Mechanical and Electronic Engineering of the University of Electronic Science and Technology of China. His research interests include condition monitoring, and fault diagnosis, signal analysis and pattern identification, mechanical vibration and machinery system dynamics.

Qiang Miao obtained B.E. and M.S. degrees from Beijing University of Aeronautics and Astronautics and Ph.D. from the University of Toronto in 2005. He is currently an Associate Professor and Chair of Department of Industrial Engineering, School of Mechanical, Electronic, and Industrial Engineering, University of Electronic Science and Technology of China, Chengdu, Sichuan, China. His current research interests include machinery condition monitoring, reliability engineering, and maintenance decision-making.